PUBLISHED BY THE INTERNATIONAL METEOROLOGICAL INSTITUTE IN STOCKHOLM

Tellus (2010), 62A, 209–217

TELLUS

The influence of synoptic scale flow on sea breeze induced surface winds and calm zones

By MARTIN GAHMBERG[1,2], HANNU SAVIJÄRVI[1]* and MATTI LESKINEN[1], [1]*Department of Physics, 00014 University of Helsinki, Finland;* [2]*WB-Sails Inc., Helsinki, Finland*

(Manuscript received 3 April 2009; in final form 2 November 2009)

ABSTRACT

High-latitude sea breezes and the related daytime calm zones were studied through fine-scale two-dimensional idealized simulations by varying the direction and speed of the ambient large-scale geostrophic flow in small steps. Strongest coastal afternoon breezes were obtained for moderate large-scale flows 45°–90° left from the pure offshore direction (as seen from the sea), while calm zones appeared near the coast for weak to moderate large-scale flows about 30°–90° right from offshore, and at the seaward edge of the breeze cell for weak ambient flows 45°–90° right from offshore. The complex daytime evolution of the wind field for ambient winds roughly opposing the sea breeze is illustrated via a few key cases.

1. Introduction

The sea breeze is a thermally induced diurnal mesoscale circulation that develops due to differential heating between land and sea via the induced pressure gradient differences. It has a major impact on the meteorological conditions at coastal areas. Hence, sea breezes have been widely investigated using observations and numerical models. For a review, see for example, Atkinson (1981), Stull (1988) and Pielke (2002).

In calm clear conditions along a straight coast with flat terrain, the sea breeze starts at the surface in the late morning perpendicularly to the shoreline, then strengthens and veers (turns to the right) in the northern mid-latitudes during the day due to the Coriolis acceleration, peaking in the afternoon (Lyons, 1972). The main environmental factors contributing to the sea breeze (and hence to the actual surface winds) are the temperature contrasts between land and sea and the quite significant effects of the synoptic-scale ambient flow interacting with the sea breeze. The main objective of the present study is the latter: we investigate the effects of the large-scale flow on the extension and intensity of the sea breeze in relation to the coastline in more detail than in earlier investigations. This is made by varying the ambient wind speed and direction in small steps in idealized high-resolution model simulations. The resulting coastal wind field can be quite complex in its daily evolution, as is illustrated.

The coastal winds are important in many applications such as local coastal weather forecasting, boat and ship traffic, ship routing by port authorities, transport and diffusion of coastal pollutants, predictions for oil slick movement with surface wind, etc. Our results may be useful for such applications and add details to the basic knowledge about sea breezes. The knowledge of the evolution of the coastal wind field (in particular wind shifts, and the location of zones of stronger and weaker winds) is of significant tactical importance also in sailing. For instance, sea breeze related calm zones were a common feature at the sailing venues in both the 2004 and 2008 Olympic Games. The information gained from the present simulations was available in 2008 and proved extremely useful for the Olympic medal-winning Swedish Star team, the first author (MG) being its coach and meteorologist. Also our other practical experience suggests that the present simulations, though idealized, still capture the essence of the subject for northern mid- and high latitudes.

The present numerical investigation was made using the University of Helsinki two-dimensional mesoscale model. Section 2 is a review of previous studies on the impact of the large-scale flow on the sea breeze. Section 3 describes the model while the results are highlighted in Section 4, concentrating only on the surface wind field for brevity and illustrating first the general aspects and then a few key cases. An observed evolution of an offshore sea breeze is presented in Section 5. It is dynamically similar to one of the key cases and validates the latter. Section 6 summarizes the findings of the numerous simulations.

*Corresponding author.
e-mail: hannu.savijarvi@helsinki.fi
DOI: 10.1111/j.1600-0870.2009.00423.x

2. Effects of background flow on the sea breeze

2.1. General effects

The ambient wind has long been known to have a significant effect on the evolution of the sea breeze. The classic two-dimensional model study by Estoque (1962) described sea breezes during 5 m s^{-1} synoptic geostrophic wind V_g from four main directions (parallel and perpendicular to the shoreline). He found that V_g from land intensifies the sea breeze by intensifying the horizontal temperature gradient from sea to land and preventing the sea breeze cell from moving inland. In contrast, an onshore background flow weakens the temperature gradient, which in turn reduces the opportunity for the development of a sea breeze. When the geostrophic wind is parallel with the coastline so that the low pressure is over the ocean, the low level frictional flow is offshore, leading to a strengthening of the temperature gradient. When the background wind blows in the opposite direction along the coast, an onshore Ekman wind component and thus a weaker circulation is induced. Similar effects of the ambient wind on the sea breeze development have been cited in many studies since (see the review by Atkinson, 1981). Estoque's model provided the basis for many later studies on the character of the sea breeze including the present one.

Arritt (1989) showed that the offshore extent of the sea breeze is greatly suppressed when the large-scale flow is onshore. In contrast, when the large-scale flow is offshore, the sea breeze perturbation extends to a considerable distance over the water. This is partly due to the fact that the background flow advects the sea breeze system offshore. The offshore synoptic-scale flow also intensifies the sea breeze perturbation by concentrating the horizontal temperature gradient at the shore, but the offshore extent of the evolving strong onshore breeze is smaller than that of a sea breeze forming in calm conditions. An offshore ambient wind of moderate speed can therefore result in a strong sea breeze front due to the increased convergence, but can, when strong enough, dominate the flow at the coast.

Atkinson (1981) and Wexler (1946) suggested that an offshore ambient wind has the effect of pushing the thermal gradient out to sea and therefore also the mesoscale pressure gradient necessary for the sea breeze. Thus the sea breeze may begin several kilometres out at sea, often not reaching the coast until mid-afternoon, if at all. Such behaviour has been observed by many others (Fisher, 1960; Frizzola and Fisher, 1963) and obtained by numerical investigations (e.g. Arritt, 1993). Observations (e.g. Atkins and Wakimoto, 1997) and numerical simulations (e.g. Arritt, 1993) further show that with an offshore ambient wind the sea breeze forms later in the day, is shallower, extends a shorter distance inland and retreats earlier than a sea breeze forming in a calm synoptic situation. In the case of an onshore large-scale wind the sea breeze tends to be hard to detect since it is weak and superposed on the onshore wind. The whole sea breeze cell also moves rapidly inland in this case (Arritt, 1993; Atkins and Wakimoto, 1997).

Arritt's (1993) results, using a two-dimensional non-linear numerical model, indicated that the thermally induced flow perturbation was already suppressed for onshore large-scale winds of a few metres per second or more, whereas an onshore component was established somewhere in the domain for opposing offshore geostrophic flows as strong as 11 m s^{-1}. A weak offshore background flow increases the sea breeze circulation, whereas a stronger flow decreases it. In Arritt's simulations the sea breeze reached the coast for offshore geostrophic winds as strong as 6 m s^{-1}. When the opposing large-scale flow was slightly stronger, there was a well-developed sea breeze circulation located entirely offshore. There is also observational evidence that sea breezes can in fact remain entirely offshore in the presence of an opposing synoptic wind (Lyons, 1972), and such a case is described in Section 5. Arritt found that the strongest sea breeze circulations are the ones that barely reach the coast in the presence of an offshore large-scale flow. This is generally consistent with Bechtold et al. (1991), who showed that the maximum sea breeze intensity near the coast is obtained when the propagation speed of the sea breeze front (about 3 m s^{-1} inland) is cancelled out by the opposite basic flow speed in the well-mixed boundary layer (in their simulations, for V_g offshore 5 m s^{-1}), leading to a stationary front.

The above findings are also consistent with Savijärvi and Alestalo's (1988) numerical study of sea breeze over lakes and sea gulfs with the extension that the sea breeze could be pushed across a sea gulf by a suitable basic flow and this may have (perhaps unexpected) impact on the opposite coast.

2.2. Sea breeze induced calm zones: onshore and offshore ends

A three-dimensional numerical simulation of the sea breeze circulation over Chesapeake Bay during an event of offshore synoptic-scale flow by Segal et al. (1982) identified regions of nearly calm winds in the onshore-end convergence zone (i.e. at the sea breeze front). These regions, which advanced gradually inland about 25 km, diminished slightly in size during the afternoon as the veering of the sea breeze reduced its opposition to the offshore flow. Clear air radar observations by Atkins and Wakimoto (1997) show that during offshore flow events, the low-level winds do tend to diminish ahead of the sea breeze front. Atkins et al. (1995) and Atkins and Wakimoto (1997) believed that this slowing-down is due to a dynamic pressure effect generated by the convergence of the two air masses. When the background flow was approximately parallel to the coast with land to the left, only a wind shift line was observed along the sea breeze front.

When the sea breeze develops during offshore large-scale flow, a calm region may also form at the seaward end of the

sea breeze cell where the breeze just balances the opposing large-scale wind. The resulting absence of sea waves makes the calm region visible from satellite images under conditions of sun glint (Fett and Tag, 1984; Langland et al., 1987). Fett and Tag showed using a two-dimensional numerical model that the position and movement of the offshore calm was quite sensitive to the ambient wind speed. Under onshore ambient flow the sea breeze merely accelerates the basic flow and calm zones do not form.

A third class of coastal sea breeze related calms was noted in Savijärvi et al. (2005) for 10 m s^{-1} ambient flow from about 250° across a west-to-east sea gulf (Gulf of Finland). In this case the strong sea breeze cell of the southern (Estonian) coast is slowly advected over the gulf so that in the late afternoon it is near the northern (Finnish) coast and its NE surface winds are just opposite to those due to the prevailing SW surface flow, so that a calm results. Such events are occasionally observed in Helsinki. They are not considered in this study, which for simplicity assumes an open sea coastline.

The ambient flow at the coast may also be provided or modified by coastal slope winds or a coastal urban heat island circulation, or both. A related sea breeze induced calm zone in the Osaka-Kyoto region has been discussed by Ohashi and Kida (2002).

Most sea breeze studies have concentrated either on case studies, or simulations with the ambient geostrophic wind V_g directly along or across the coast. Our contribution is to chart systematically all directions and several speeds of V_g.

3. The numerical model and set-up of the experiments

We investigate the effects of the large-scale flow on the sea breeze near the coastline at 60°N using the University of Helsinki (UH) mesoscale model. This model has closely reproduced the observed average calm weather sea breeze in Helsinki, as well as the strong surface easterlies associated with sea breezes during moderate to strong southeasterly basic flow (Savijärvi et al., 2005). It has also simulated subtropical and tropical sea breezes in considerable detail (Savijärvi, 1995; 1997; Savijärvi and Matthews, 2004).

The UH model is a two-dimensional moist sigma coordinate model with the dynamic core from Alpert et al. (1982) and Alpert and Savijärvi (2008). The active physical parametrizations include in the present experiments a Monin-Obukhov surface layer, a Blackadar-type first-order mixing length turbulence closure, a force-restore scheme for soil temperatures, and a comprehensive radiation scheme with six bands in the long-wave and four in the short wave. Clouds did not form. Free-flow horizontal boundary conditions are applied. The model equations, numerical details and parametrizations are described in the above references and references therein.

The version used in this study involves 65 grid points and 11 levels. The two lowest levels are at heights of about 2 and 10 m above the surface, while the model top is at 4.5 km. Horizontal grid lengths of 1, 2, 4 and 8 km were used. The set-up is across a straight, open sea coastline at 60°N with flat forested land in the north during a typical clear-sky early summer day in southern Finland. The sea surface temperature is kept at 13 °C while the predicted inland afternoon 2 m temperatures reach the realistic 20–23 °C (depending on the winds). The model assumes a steady large-scale pressure gradient in the form of a geostrophic wind, which is here constant in space and time during each simulation. The direction of the geostrophic wind was varied by steps of 11.25°, and the speed with steps of 1 m s^{-1}; the results are shown for V_g of 4 and 7 m s^{-1}. The simulations were run from 04 to 22 local solar time (LST) from an initial state of 13 °C at the surface with the lapse rate of 6.5 K km^{-1} and relative humidity of 50%. The coastline is for convenience aligned in the east–west direction with land to the north, so that a southerly wind vector (180°) corresponds to the flow directed from sea to land. In this study the surface winds refer to 10 m height, and winds under 1 m s^{-1} are considered as calm.

At about 05 LST the horizontal temperature gradient is still negligible, but the surface winds have adjusted to the local roughness of each grid point (z_o 1 mm over the sea, 50 cm over forested land). Thus the 05 LST surface wind field is a good indicator of winds without any sea breeze, and would effectively prevail all day in an overcast simulation. The details of such coastal afternoon wind fields were studied in Savijärvi (2004).

4. Model results

The results shown are obtained from simulations using a grid length of 2 km. (Many cases were also run using grid lengths of 1 and 4 km; these resulted in nearly identical wind patterns with only small spatial and temporal differences.) For reference, in the absence of any geostrophic wind the obtained 15 LST 'pure' 10 m sea breeze is 4.5 m s^{-1} from SW (215–220°) at the sea points 2–6 km from the coast, veering to 2 m s^{-1} WSW (255°) by 21 LST. As discussed in Savijärvi et al. (2005), this breeze, its return flow at about 2 km height, the inland SB cell movement of about 3 m s^{-1}, and its evolution are similar to the average of observed calm case sea breezes in Helsinki.

Even for very light (1–2 m s^{-1}) geostrophic winds, the UH model produces quite variable sea breeze patterns depending on the direction of the background flow, which advects the SB cell and modifies the associated surface heat transfer and mesoscale pressure gradient patterns driving the sea breeze, as discussed in Section 2. These very light geostrophic wind cases have characteristics similar to the cases with stronger background flows described below, only with smaller amplitude.

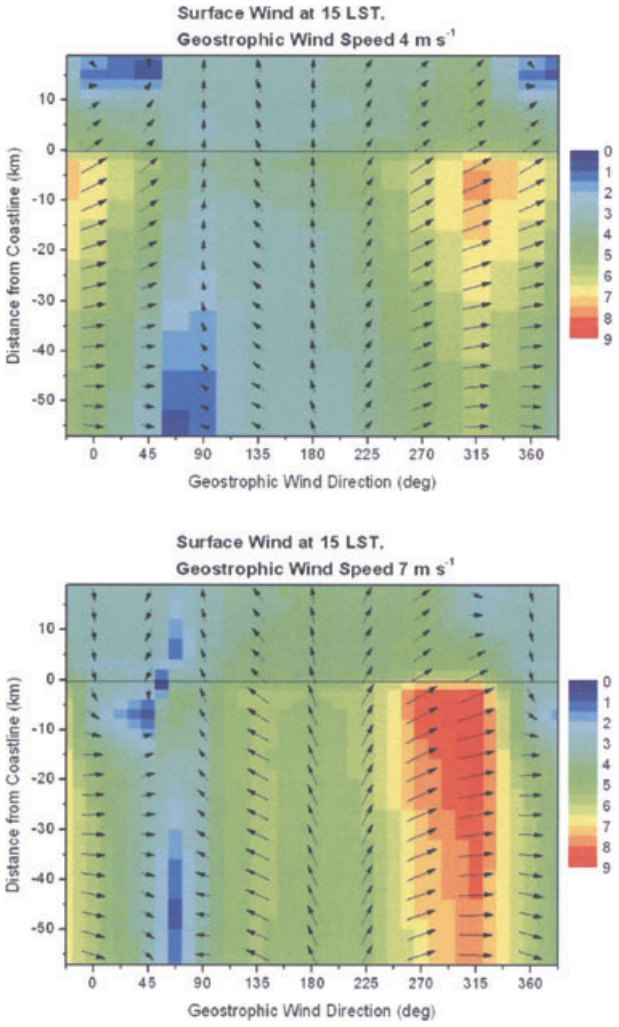

Fig. 1. The model-predicted surface wind vectors (speed also in colour scale, m s^{-1}) at 15 LST as a function of geostrophic wind direction (°) and distance from the coast (km, negative values at the sea), for geostrophic wind speeds of 4 m s^{-1} (upper panel) and 7 m s^{-1} (lower panel). Land is in the north; the pure onshore direction is 180°.

4.1. An overall picture of the model-predicted sea breeze intensity

The general influence of the geostrophic wind on the afternoon coastal winds is summarized in Fig. 1, which also indicates the extension and intensity of the sea breeze cell near the surface. Figure 1 displays the 10 m wind vectors at 15 LST as a function of the distance from the coast and the direction of the prevailing geostrophic wind. Two geostrophic wind speeds are displayed. During a light ambient flow (V_g4 m s^{-1}, upper panel) the strongest surface winds, sea breezes of 7.5–8 m s^{-1} from WSW, are obtained at 2–17 km off the coast for geostrophic winds slightly backed (left-hand side) from the pure offshore direction, V_g being from NW or 315°. These SW breezes extend far inland and also far out to the sea. When the background flow is increased to moderate (V_g 7 m s^{-1}, lower panel), the strongest breezes (red) are up to 9–9.5 m s^{-1} for V_g from NW to WNW but here the breezes extend only about 10 km inland at 15 LST. For the even stronger V_g of 10 m s^{-1} from W (not shown) the coastal surface winds can exceed 10 m s^{-1} (Savijärvi et al., 2005).

The offshore V_g from the NW sector thus favours strong sea breezes by keeping the SB cell and the driving temperature and pressure contrasts near the coast. Another reason for the relatively strong surface winds is that vectors of the SB component and that of the frictionally turned surface wind due to the prevailing NW flow tend to add constructively. On the other hand all onshore ambient winds (V_g from the S sector in Fig. 1) advect the emerging SB cell rapidly inland so no afternoon SB is seen near the coast.

The wind speed minima (blue) are also evident in Fig. 1. During light offshore V_g from N to NE the sea breeze front with the associated surface wind speed minimum is located 15–20 km inland at 15 LST (upper panel). Moderate 7 m s^{-1} V_g from the NE sector has pushed the breeze cell to the sea (lower panel); hence the front (the SB convergence zone) is right above or near the coastline. Note how sensitive the actual location of this afternoon calm is to but small changes in the direction of a moderate V_g, according to Fig. 1. The effect of the speed of V_g can be roughly estimated by comparing the upper and lower panels.

For light V_g from the E–NE sector, also the seaward end calm zone of a weak sea breeze cell can be noted well out at the sea in Fig. 1. During a stronger ambient wind it is only discernible for V_g from ENE. The horizontal extent of the SB cell is fairly small in this case. The sensitivity of this seaward calm to the prevailing flow was already noted by Fett and Tag (1984).

In Fig. 2, the surface wind vectors at 05 LST have been subtracted from winds at 15 LST at each grid point and the wind speeds of the difference are plotted. In other words, the intensity of the sea breeze perturbation (and weaker effects of stronger vertical mixing of momentum over land at 15 LST versus 05 LST) can be seen in Fig 2. During a light background flow (upper panel) the strongest sea breeze perturbation is obtained for V_g from N to NE. Here the cool sea breeze and the ambient flow from warm land have opposite directions in the lower boundary layer, leading to strong and stationary horizontal temperature gradients and hence to a strong and long-lasting sea breeze. In contrast, during an onshore ambient flow (V_g from S) the sea breeze perturbation remains small.

When the background flow is increased to 7 m s^{-1} (lower panel), V_g from N (directly offshore) advects the sea breeze perturbation well out to the sea by 15 LST, so the perturbations are actually strongest for V_g to the right (NE–ENE) and left (NW) from the pure offshore direction. In these directions the offshore component of the geostrophic flow is optimal, around

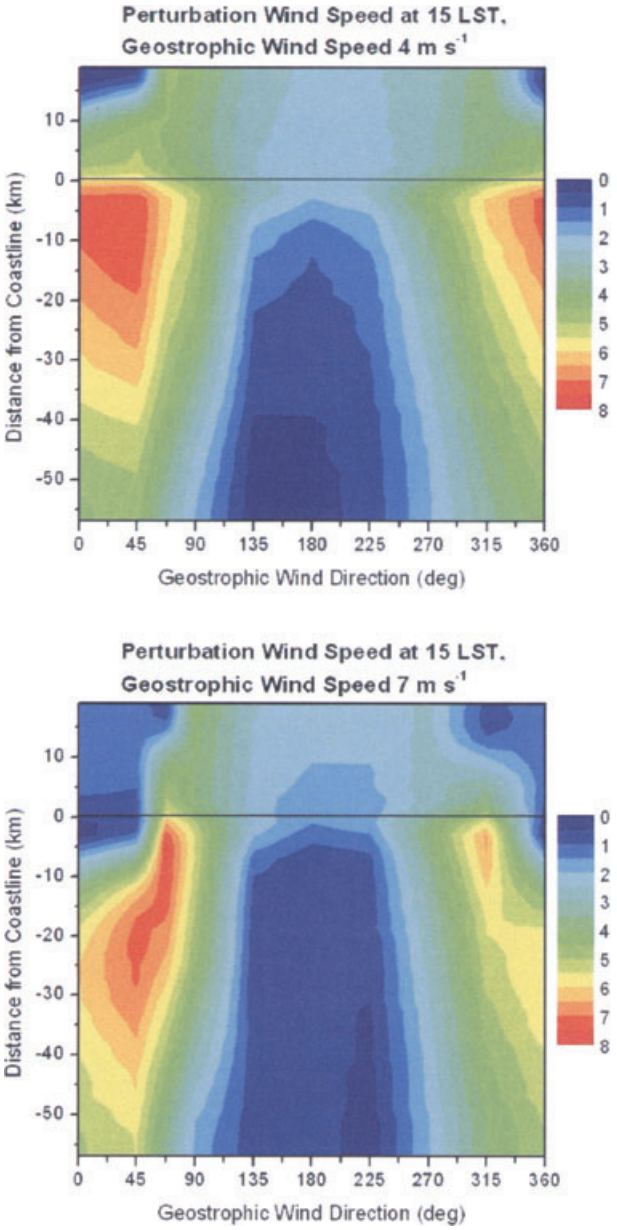

Fig. 2. As Fig. 1 but for wind speeds of perturbations from the 05 LST wind.

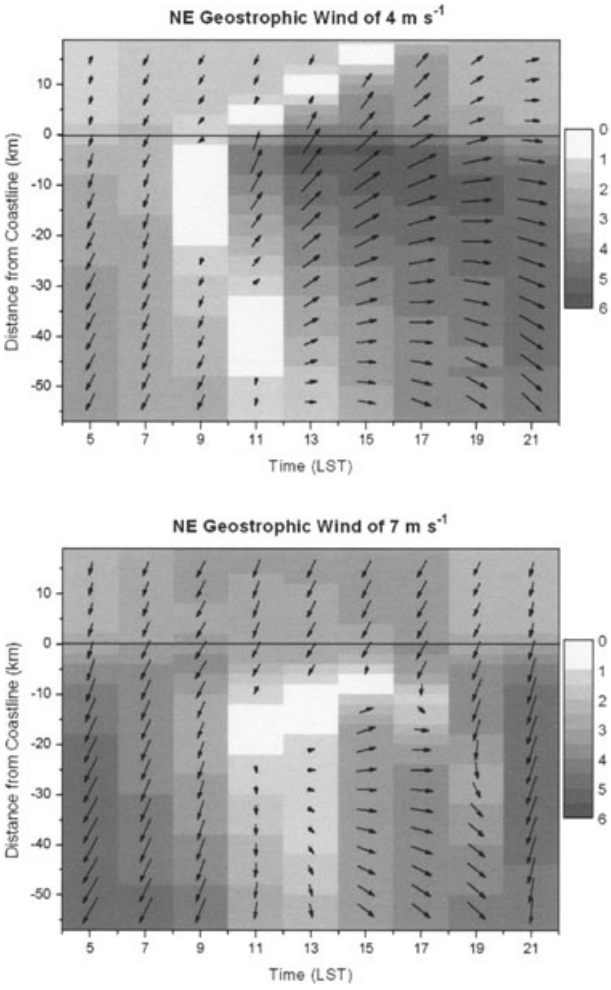

Fig. 3. Model-predicted surface wind vectors (speed also in grey scale, m s^{-1}) as a function of local solar time (LST) and distance from the coast (km, negative values at the sea), for geostrophic winds from NE (45°) with speed of 4 m s^{-1} (upper panel), 7 m s^{-1} (lower panel).

5 m s^{-1}, for a strong sea breeze perturbation, as found by Estoque (1962) and others. The complete calm 5–10 km out at the sea for moderate V_g from NE in Fig. 1 is thus associated with the sea breeze perturbation being strong 20 km offshore in Fig. 2. For the stronger V_g of 10 m s^{-1} Savijärvi et al. (2005) obtained the calmest near-coast afternoon winds during V_g from 79°, when the strong SW sea breeze perturbation and the frictionally turned NE surface wind of the large-scale flow were nearly opposite just above the coastline.

4.2. *Examples of the evolution of the sea breezes and related calm zones*

Some key cases are now discussed. They are associated with geostrophic winds blowing from the NE quadrant in our set-up, since for other directions of V_g the afternoon coastal wind field is less variable, according to Fig. 1.

Figure 3 displays the daytime evolution of the surface wind field for V_g from NE. At 05 and 07 LST there is no sea breeze as yet; instead one can recognize slightly stronger surface winds over the smooth sea than over the rough land. During light V_g (upper panel) a weak sea breeze has been triggered 5–20 km out at the sea at 09 LST but it is compensated by the opposite basic flow, so that the resulting total surface wind appears calm in Fig. 3. By 11 LST there is a narrow strip of SSW sea breezes just off the coast. The related convergent frontal and divergent seaward edge calm zones are clearly visible 3–6 km inland and

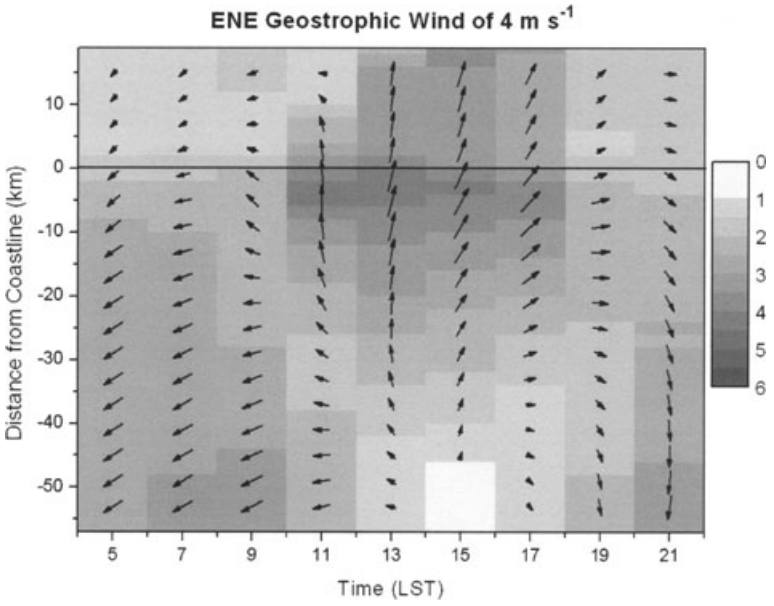

Fig. 4. As Fig. 3, but for geostrophic wind of 4 m s^{-1} from ENE (68°).

33–48 km out to the sea respectively. At 13 LST the SW sea breezes are 5–6 m s^{-1} over the coastal waters. The frontal calm is now located about 8 km inland while the seaward edge calm is best seen in the form of weak westerly winds far at the sea. At 15 LST the front has advanced 15 km inland, the zone of moderate sea breezes at the sea is broad while the seaward edge calm has more or less disappeared. Towards the evening the sea breeze cell is pushed more and more seaward by the prevailing light NE flow, surface winds veering to westerlies and then to weak land breezes.

With the stronger advecting V_g from NE (lower panel), the emergence of the sea breeze cell is delayed to 11 LST. It now remains all day at the sea, the frontal calm zone being about 5–10 km off the shore in the afternoon. As with Fig. 1, comparison of the upper and lower panels of Fig. 3 vividly demonstrates the effect of the large-scale flow speed. For instance, it can be estimated that the calm zone will prevail right over the coastline during midday and early afternoon for northeasterly V_g of about 6 m s^{-1}.

Figure 4 demonstrates the evolution of surface winds in a case where the midday and early afternoon winds veer steadily and are at their strongest right at the coast, getting weaker seaward. V_g is here 4 m s^{-1} from ENE (68°). The sea breeze cell advances inland during the afternoon due to the small resisting offshore component (1.5 m s^{-1}) of the light basic ENE flow.

In contrast, the behaviour of the coastal wind is very different for V_g of 7 m s^{-1} from NE to ENE (56°). This case is illustrated in Fig. 5. Here the frontal calm is located immediately off the coastline all afternoon. Wind speeds now increase seaward but their directions are, perhaps unexpectedly, directly opposite to those observed at the same time over land and even at the coastline. In the early morning the coastal surface winds are weak northeasterlies just as in Fig. 4, but the sea breeze cell never enters land in the case of Fig. 5, as the offshore component of the advecting basic flow, 3.9 m s^{-1}, is stronger than the inland drift (about 3 m s^{-1}) of the SB cell. At 13 LST both the frontal and the seaward edge calms are clearly recognizable in Fig. 5.

Hence even small changes in the prevailing flow can make dramatic differences to the actual wind patterns at the coastal waters. The present simulations appear to confirm all the previous results and physics discussed in Section 2 while adding new details into the broad picture.

5. Observational evidence of an offshore sea breeze

As a verification of the existence of offshore sea breezes, we consider the case of 2002 September 11, when the synoptic observations at the island weather station Isosaari (25.0°E, 60.1°N) 8 km south of Helsinki indicated that northeasterly surface winds prevailed during the sunny morning and midday (Table 1). At 12 UTC (about 14 LST) the winds were nearly calm before a southwesterly sea breeze arrived, which was observed at 15 UTC. The sea breeze vanished by 18 UTC as the winds shifted back to the north. Observations at Helsinki-Vantaa (about 10 km inland) and Helsinki-Kaisaniemi (at the virtual coastline) indicate that the sea breeze never reached the shore and northerly surface winds prevailed all day. The coastline of southern Finland runs WSW–ENE. Hence these surface observations and surface pressure analyses indicate that the prevailing afternoon low-level geostrophic wind, about 7 m s^{-1} from 30°, was about 45° to the right of the pure offshore direction and so the situation is dynamically similar to our simulation shown in the lower panel of Fig. 3 (moderate V_g from NE).

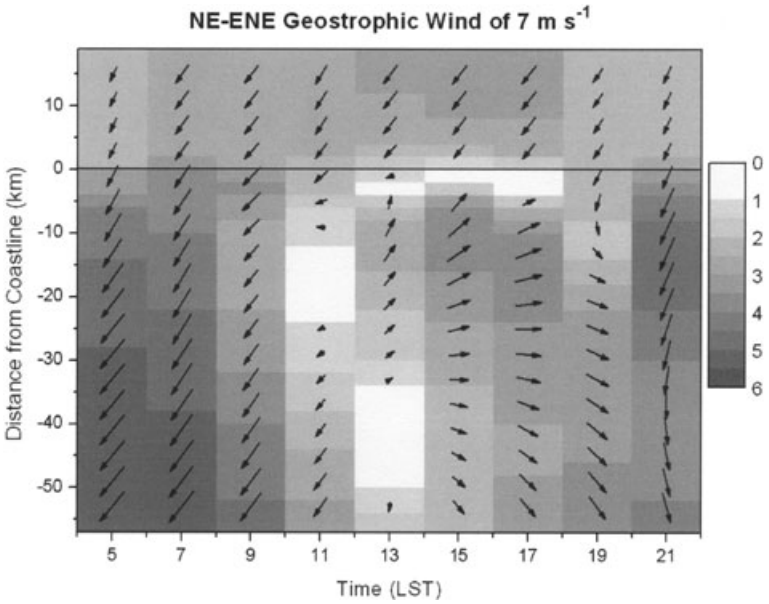

Fig. 5. As Fig. 3, but for geostrophic wind of 7 m s^{-1} from NE to ENE (56°).

Table 1. Surface wind observations at three synoptic stations across Helsinki for 11 September 2002 (Finnish Meteorological Institute statistics).

	03 UTC	06 UTC	09 UTC	12 UTC	15 UTC	18 UTC	21 UTC
Vantaa	20°	30°	0°	330°	340°	340°	0°
(10km inland)	2 m s^{-1}	3 m s^{-1}	4 m s^{-1}	4 m s^{-1}	5 m s^{-1}	2 m s^{-1}	0 m s^{-1}
Kaisaniemi	20°	50°	20°	350°	350°	340°	10°
(coastline)	2 m s^{-1}	2 m s^{-1}	3 m s^{-1}	3 m s^{-1}	3 m s^{-1}	2 m s^{-1}	1 m s^{-1}
Isosaari	40°	40°	50°	120°	230°	350°	10°
(8 km offshore)	6 m s^{-1}	5 m s^{-1}	3 m s^{-1}	1 m s^{-1}	5 m s^{-1}	5 m s^{-1}	2 m s^{-1}

Clear air insect echo radar images obtained by the University of Helsinki Doppler weather radar are presented in Fig. 6. The radar was located in the centre of Helsinki at the virtual coastline and next to the Kaisaniemi weather station. Figure 6 displays vertical cross sections of the radial wind component toward the sea and Isosaari (azimuth 156.6°) at 1135 and 1235 UTC. These radar images show that a shallow sea breeze (blue: wind toward radar at the coast) existed entirely over the water in a northerly flow (red and green: wind away from radar and coast) with a return flow maximum aloft. The leading edge of the sea breeze moved over Isosaari (8 km offshore) at about 1200 UTC (14 LST), which is also when the wind minimum was observed at this weather station (Table 1). These observations fit surprisingly well with the idealized simulation shown in the lower panel of Fig. 3.

6. Conclusions

Our objective was to study the effect of geostrophic winds on the surface level sea breeze and the induced calm regions near the coast. Previous investigations were reviewed and the University of Helsinki mesoscale model was used to examine in detail the sea breeze phase of the surface flow as a function of the geostrophic wind. The simulations indicate that the development of the sea breeze and the appearances of sea breeze induced calm zones can be highly sensitive to small changes in the direction and magnitude of the prevailing geostrophic wind, particularly in the quadrant right from the pure offshore direction (in the northern hemisphere). The interaction of the sea breeze with the synoptic wind may create a complex spatial and temporal flow pattern at the coast.

An offshore-directed component of the synoptic-scale flow intensifies the sea breeze perturbation by concentrating the horizontal temperature gradient, whereas even a weak onshore flow greatly reduces the possibility of the development of a sea breeze. The perturbation is on the other hand suppressed when the offshore background flow is strong enough. The temperature gradient and the associated sea breeze perturbation is pushed out to sea in the presence of an offshore background flow component stronger than about 3 m s^{-1}. Hence, the sea breeze may start several kilometres out to sea and may remain entirely over the water. An observed case is discussed in Section 5.

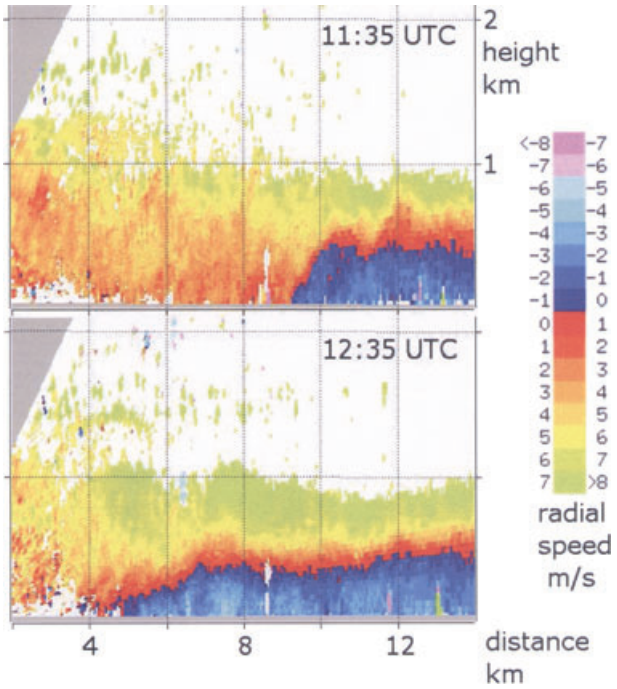

Fig. 6. Vertical cross-sections 0–2 km of Doppler radial wind speeds (m s^{-1}) to 156.6° (offshore) from the University of Helsinki weather radar at 1135 UTC (upper panel) and 1235 UTC (lower panel) on September 11, 2002. Onshore winds are blue (i.e. toward the radar), offshore winds red-orange-green. Note the advancing sea breeze.

Previous numerical simulations and observations (e.g. Segal et al., 1982; Fett and Tag, 1984; Arritt, 1993; Atkins et al., 1995; Atkins and Wakimoto, 1997) furthermore show that when a sea breeze develops in the presence of an offshore synoptic-scale flow, wind speed minima may appear just ahead of the sea breeze front or at the offshore end where the sea breeze just balances the opposite large-scale wind. The veering of the sea breeze, due to the Coriolis effect, may diminish the opposition of the sea breeze to the basic flow and lead to a less pronounced wind speed minimum at the front. The wind speed minima at the offshore end are more obvious for lighter opposing large-scale flows.

The present simulations agree with the above previous findings and add a more detailed picture of the interaction between the offshore basic flow and the sea breeze. Weak to moderate offshore basic flows can be divided into four sectors with typical characteristics of the surface winds over the coastal waters summarized as follows.

(1) Ambient flows left from the offshore direction (as seen from the sea) produce the strongest afternoon surface winds (Fig. 1). The coastal winds back up in the beginning of the day as the sea breeze perturbation grows, but later on the winds veer toward the synoptic-scale direction, due to the Coriolis effects and the weakening sea breeze circulation. In these cases only a wind shift line appears at the leading edge of the circulation.

(2) For geostrophic winds about 0–30° right from the offshore direction a clear wind speed minimum appears in front of the evolving sea breeze. When the geostrophic direction is close to 30°, a calm strip appears at the leading edge of the sea breeze. The turning of the surface winds, affected by the sea breeze perturbation, is anticlockwise in the beginning of the breeze period and later clockwise.

(3) For the geostrophic wind directions about 30–60° right from the offshore direction the midday sea breeze is opposed in direction to the surface basic flow. In the morning the thermally induced perturbations initially create a wide calm zone offshore for geostrophic winds lighter than about 7 m s^{-1}. In this calm region an onshore breeze develops, dividing the initial calm into two separate calm zones, one ahead and the other behind the sea breeze. This breeze only turns clockwise during the day (Fig. 3). Due to the Coriolis effect and the more westerly direction of the sea breeze perturbation at the seaward end, the calm at the offshore end disappears much earlier than the frontal calm. A background flow of larger magnitude or a direction more from the left leads to a less obvious wind speed minimum behind the sea breeze (Figs. 3 and 5).

(4) When the geostrophic wind is from 60 to 100° right from the pure offshore direction, a calm zone behind the sea breeze may appear relatively late in the afternoon after the sea breeze perturbation has veered enough to cancel out the basic flow (Fig. 4). When the basic flow is weak and nearly parallel with the coast (low pressure over the sea), a calm zone appears out to the sea in the late afternoon and moves inland during the evening.

Strong (10 m s^{-1}) geostrophic winds 0–60° right from the offshore direction swamp the sea breeze and only offshore winds are present at the surface during the day. The wind far out to sea however decelerates due to the sea breeze perturbations which have been pushed offshore. In the case of a strong geostrophic wind directed 70–80° right from offshore, the surface winds can be largely cancelled out at the sea in the late afternoon due to the sea breeze effect.

The relatively strong high-latitude Coriolis force contributes in our study to the rapid veering of the sea breeze during the day and evening (Yan and Anthes, 1987). This in part makes the appearance of the calm zones and the behaviour of the surface flow rather complex and sensitive to small changes of V_g.

References

Alpert, P. and Savijärvi, H. 2008. On the numerical asymmetry in calculating Coriolis terms through the splitting method in a mesoscale model. *Int. J. Environ. Pollut.* **32**, 139–148.

Alpert, P., Cohen, A., Neumann, J. and Doron E. 1982. A model simulation of the summer circulation from the eastern Mediterranean past Lake Kinneret in the Jordan Valley. *Mon. Wea. Rev.* **110**, 994–1006.

Arritt, R. W. 1989. Numerical modeling of the offshore extent of sea breezes. *Quart. J. Roy. Meteor. Soc.* **115**, 547–570.

Arritt, R. W. 1993. Effects of the large-scale flow on characteristic features of the Sea Breeze. *J. Appl. Meteor.* **32**, 116–125.

Atkins, N. T. and Wakimoto, R. M. 1997. Influence of the synoptic-scale flow on sea breezes observed during CaPE. *Mon. Wea. Rev.* **125**, 2112–2130.

Atkins, N. T, Wakimoto, R. M. and Weckwerth, T. M. 1995. Observations of the sea breeze front during CaPE. Part II: dual doppler and aircraft analysis. *Mon. Wea. Rev.* **123**, 944–969.

Atkinson, B. W. 1981. *Meso-Scale Atmospheric Circulations*. Academic Press, London, UK, 496 pp.

Bechtold, P., Pinty, J.-P. and Mascart, P. 1991. A Numerical Investigation of the Influence of Large-Scale Winds on Sea-Breeze- and Inland-Breeze-type Circulations. *J. Atmos. Sci.* **30**, 1268–1279.

Estoque, M. A. 1962. The sea breeze as a function of prevailing synoptic situation. *J. Atmos. Sci.* **19**, 244–250.

Fett, R. W. and Tag, P. M. 1984. The sea-breeze-induced coastal calm zone as revealed by satellite data and simulated by a numerical model. *Mon. Wea. Rev.* **112**, 1226–1233.

Fisher, E. L. 1960. An observational study of the sea breeze. *J. Met.* **17**, 645–660.

Frizzola, J. A. and Fisher, E. L. 1963. A series of sea-breeze observations in the New York City area. *J. Appl. Met.* **2**, 722–739.

Langland, R. H., Tag, P. M. and Fett, R. W. 1987. Numerical simulation of a satellite-observed calm zone in Monterey Bay, California. *Wea. Forecast.* **2**, 261–268.

Lyons, W. A. 1972. The Climatology and Prediction of the Chicago Lake Breeze. *J. Appl. Meteor.* **11**, 1259–1270.

Ohashi, Y. and Kida, H. 2002. Effects of mountains and urban areas on daytime local-circulations in the Osaka and Kyoto regions. *J. Met. Soc. Japan* **80**, 539–560.

Pielke, R. A. 2002. *Mesoscale Meteorological Modelling* 2nd Edition. Academic Press, San Diego.

Savijärvi, H. 1995. Sea breeze effects on large-scale atmospheric flow. *Contr. Atmos. Phys.* **68**, 335–344.

Savijärvi, H. 1997. Diurnal winds around Lake Tanganyika. *Quart. J. Roy. Meteor. Soc.* **123**, 901–918.

Savijärvi, H. 2004. Model predictions of coastal winds in a small scale. *Tellus* **56A**, 287–295.

Savijärvi, H. and Alestalo, M. 1988. The sea breeze over a lake or gulf as the function of the prevailing flow. *Beitr. Phys. Atmos.* **61**, 98–104.

Savijärvi, H. and Matthews, S. 2004. Flow over small heat islands: a numerical sensitivity study. *J. Atmos. Sci.* **61**, 859–868.

Savijärvi, H., Niemelä, S. and Tisler, P. 2005. Coastal winds and low-level jets: simulations for sea gulfs. *Quart. J. Roy. Meteor. Soc.* **131**, 625–637.

Segal, M., McNider, R. T., Pielke, R. A. and McDougal, D. S. 1982. A numerical model simulation of the regional air pollution meteorology of the Greater Chesapeake Bay area—summer day case study. *Atmos. Environ.* **16**, 1381–1397.

Stull, R. B. 1988. *An Introduction to Boundary Layer Meteorology*. Kluwer, Dordrecht, The Netherlands.

Wexler, R. 1946. Theory and observations of land and sea breezes. *Bull. Am. Meteor. Soc.* **27**, 272–287.

Yan, H. and Anthes, R. A. 1987. The effect of latitude on the sea breeze. *Mon. Wea. Rev.* **115**, 936–956.